

The role of polymer spacers in specific adhesion

André G. Moreira^{a)}

Materials Research Laboratory, University of California, Santa Barbara, California 93106

Carlos M. Marques

LDFC-CNRS UMR 7506, 3 rue de l'Université, 67084 Strasbourg Cedex, France

(Received 16 July 2003; accepted 7 January 2004)

We study the role of flexible spacers in specific adhesion from the point of view of polymer reaction–diffusion theory. By assuming that the interactions between complementary adhesion moieties occur on a length scale much smaller than the size of the polymer spacer, we describe in detail binding and rupture between two opposing surfaces. Predictions are given for the physical properties of interest such as the time evolution of bond density and the ranges of attraction and unbinding. We also discuss the dynamic crossover between reversible and irreversible bridging.

© 2004 American Institute of Physics. [DOI: 10.1063/1.1651088]

I. INTRODUCTION

Biotin and streptavidin are standard examples of ligand–receptor pairs that give rise to specific adhesion.^{1,2} Measurements of binding free energy^{3,4} have provided values in the range $30\text{--}35 k_B T$, almost as large as 1 eV, the typical energy of covalent bonds. Although such strong interactions only rarely occur in nature, a broad spectrum of molecules² exist that provide for specific, complementary interactions in the range $1\text{--}20 k_B T$, see for instance Table I. Moreover, the interaction between the ligand receptor pairs is typically short ranged.^{5,6} For the biotin–streptavidin case, for instance, only when the distance from the biotin to the streptavidin site is smaller than 1 nm can any adhesiveness be felt. In practical situations, the ligands and receptors promote adhesion between two opposing surfaces to which they are attached.^{7–9} The specificity of these stickers, requiring a well-defined relative positioning of the molecules for the interaction to occur, implies a low effective affinity between the opposing surfaces if at least one of the moieties has not kept some mobility. Flexible molecules that anchor the ligand or the receptor to the surface, while providing for such mobility, are called spacers. They play a central role^{10–15} in controlling the adhesion between two surfaces by tuning the binding range and kinetics of ligand–receptor pairs.

Flexible and semi flexible polymers are good candidates to mimic the behavior of natural spacers, and as such, they are employed in experiments on model systems.^{16–18} Early work^{19–21} on the role of spacers on specific adhesion has assumed that they can be modeled as single springs in a viscous environment, with one spring constant k and the associate relaxation time $\tau = \zeta/k$, with ζ the viscous friction coefficient. Although this is a reasonable starting point, such simplified representation of a linear molecule, with many configurational degrees of freedom, does not accurately describe the movement of the actual polymer spacers. It is well known, for instance, that the end monomer of a polymer

chain does not follow a simple diffusion trajectory, even at short times,²² contrary to the movement of a particle attached to a single spring. The modeling of a polymer chain by a single spring has been shown to wrongly predict many features of the kinetics of polymer reactions.²³

In this paper we describe the bridging kinetics of polymer spacers, by properly accounting for the many internal dynamic modes of the chains within the framework of polymer reaction–diffusion (RD) theory. A summary of some of the calculations and results reported here were announced in a previous letter.²⁴ In the next section we revisit classical results of this formalism, and extend it to account for the possibility of reversible reactions, where both binding and unbinding can occur. The case of reactions occurring during the diffusion of a particle tethered to a single spring is fully discussed for later reference. A number of new analytical results are presented in this context. In Sec. III we discuss the kinetics of polymer spacers, and describe both the binding process of two surfaces moving towards each other and the rupture of two surfaces being separated. Finally, in the conclusions we discuss the experimental relevance of our results and speculate on possible new developments of our formalism.

II. THE REACTION–DIFFUSION EQUATION

We consider a system of noninteracting mobile particles, the ligands, and fixed reaction sites, the receptors. When a ligand moves into the reaction range of the receptor, a reversible or irreversible reaction takes place. The absence of interactions between ligands implies that the joint spatial probability distribution of the ligands at time t is the product of single ligand spatial probability distributions $\Psi(\mathbf{r}, t)$. Under such conditions, the knowledge of $\Psi(\mathbf{r}, t)$ is enough to describe the system. The latter is governed by the reaction–diffusion equation

$$\mathcal{L}\Psi(\mathbf{r}, t) = -Q(\mathbf{r}, t)\Psi(\mathbf{r}, t) + P(\mathbf{r}, t) \left[1 - \int d\mathbf{r}' \Psi(\mathbf{r}', t) \right] \quad (1)$$

^{a)}Present address: BASF AG Polymer Physics, 67056 Ludwigshafen, Germany.

TABLE I. Binding free energy data for some ligand–receptor pairs. The free energy of binding can be in some cases of the order of $k_B T$, making the inclusion of reversibility in the reaction relevant for biological systems. Data from Weber (Ref. 2).

Protein	Ligand	Binding free energy ($k_B T$)
Streptavidin	Biotin	–32
Anti-DNP-globulin	DNP-lysine	–14––20
Horse liver ADH	NADH	–15
Yeast ADH	Ethanol	–4.2

with \mathcal{L} an operator. In the case of free diffusing ligands, for instance, \mathcal{L} is the diffusion operator

$$\mathcal{L} = \frac{\partial}{\partial t} - D \nabla^2, \quad (2)$$

where D is the diffusion coefficient. In the presence of any external potential acting on the ligands, \mathcal{L} becomes a Fokker–Planck (FP) operator, i.e., $\mathcal{L}\Psi=0$ is the FP equation for the problem.²⁵

The details of the reaction between receptors and ligands are contained in Q . In particular, Q carries information about the location of the reaction sites and capture radius. The product $Q\Psi$ gives the probability rate of reaction between ligands and receptors. In other words, the first term on the right-hand side (rhs) of Eq. (1) decreases the spatial integral of Ψ whenever some ligand travels to within the reaction radius of a receptor, which effectively removes ligands from

the system. Obviously, the latter also means that receptors are removed from the system. However, we assume in this work that the number of available receptors largely exceed the number of ligands, in which case this effect is irrelevant. The second term on the rhs of Eq. (1), containing P , describes the process of reverse reaction, i.e., a rupture event in a ligand–receptor complex previously formed. Such rupture occurs through thermal activation, and it releases a ligand back to the system thus increasing the value of the spatial integral of Ψ .

We will restrict here our treatment to homogeneous distributions of receptors on flat surfaces. In this case, only z , the dimension perpendicular to the surface is relevant, and the system is one dimensional. The spatial probability distribution $\psi(z, t)$ is a function of z and time t only, and Eq. (1) can be rewritten as

$$\mathcal{L}_1 \psi(z, t) = -Q(z, t) \psi(z, t) + P(z, t) \left[1 - \int dz \Psi(z, t) \right], \quad (3)$$

where now \mathcal{L}_1 is the corresponding one dimensional, diffusion or FP operator. Since Eq. (3) is linear, one can formally solve it using the Green's function method.²⁶ The propagator G follows from the solution of the equation

$$\mathcal{L}_1 G(z, z', t - t') = \delta(z - z') \delta(t - t') \quad (4)$$

with the appropriate boundary conditions specific to the system. Notice that G is the conditional probability of finding a ligand at a position z' at time t' provided that it was at z at time t . Using Eqs. (3) and (4), it follows that

$$\psi(z, t) = \psi_0(z, t) + \int_0^t dt' \int dz' G(z, z', t - t') \left[-Q(z', t') \psi(z', t') + P(z', t') \left[1 - \int dz'' \psi(z'', t') \right] \right], \quad (5)$$

where $\psi_0(z, t)$ is the solution of the diffusion or FP equation in the absence of reaction, i.e., $\mathcal{L}_1 \psi_0(z, t) = 0$. The advantage of this formal integral solution for ψ is that, for systems like polymer chains, with many internal modes, it is easier to formulate explicitly the propagator G than writing down the problem in terms of the operator \mathcal{L}_1 .^{27,28}

The homogeneous distribution of receptors on a flat surface located at position $z = \ell$, and the short range reaction radius, are expressed by the following sink and source operators Q and P :

$$Q(z, t) = q \delta(z - \ell) \quad (6)$$

and

$$P(z, t) = p \delta(z - \ell). \quad (7)$$

The delta function is well adapted to describe a structureless reaction sink, a good approximation for typical ligand–receptor interaction ranges that are short in comparison to the spatial variation of the external potential imposed upon the ligand. More complex potentials can also be accounted for by this formalism, for instance by combining several delta

functions, but the exploration of those fine effects is beyond the scope of the present work. A simple dimensional analysis of Eq. (1), using Eqs. (6) and (7), reveals that q has dimensions of a velocity (length/time), while p the dimensions of a frequency (inverse time). At a later stage, we will take the limit $p \rightarrow \infty$ and $q \rightarrow \infty$, while keeping the ratio q/p finite. This limit roughly amounts to making both the forward and backward reactions infinitely fast, while keeping a finite reaction radius.

Plugging Eqs. (6) and (7) into Eq. (5) leads to

$$\psi(z, t) = \psi_0(z) + \int_0^t dt' G(z, \ell; t - t') \times [-q \psi(\ell, t') + p \phi(t')], \quad (8)$$

where

$$\phi(t) = 1 - \int dz \psi(z, t). \quad (9)$$

This quantity, $\phi(t)$, represents the fraction of reacted ligands, and as such, it is of central importance for our de-

scription. Since the integral over t' in Eq. (8) is a convolution, it is convenient to introduce the Laplace transform

$$\hat{f}(s) \equiv \int_0^\infty dt f(t) \exp\{-st\} \quad (10)$$

and write the reaction–diffusion equation as

$$\hat{\psi}(z, s) = \frac{\psi_0(z)}{s} + \hat{G}(z, \ell, s)(-q\hat{\psi}(\ell, s) + p\hat{\phi}(s)). \quad (11)$$

Integrating Eq. (11) in z and using Eq. (9) yields

$$s\hat{\phi}(s) = q\hat{\psi}(\ell, s) - p\hat{\phi}(s). \quad (12)$$

Evaluating Eq. (11) at $z = \ell$ leads to a self-consistent relation between $\psi(\ell, t)$ and $\phi(t)$. Plugging the latter result into Eq. (12) and taking the limit of fast reactions ($p \rightarrow \infty$, $q \rightarrow \infty$ and $k \equiv q/p$ finite) one finally obtains, after some algebra,

$$\hat{\phi}(s) = \frac{1}{s} \frac{k\psi_0(\ell)}{1 + ks\hat{G}(\ell, \ell, s)}. \quad (13)$$

In the limit $s \rightarrow 0$ (which corresponds to $t \rightarrow \infty$), the dynamic propagator reduces to the equilibrium probability distribution in the absence of reaction, i.e., $\hat{G}(\ell, \ell, s) \rightarrow \psi_0(\ell)/s$ as $s \rightarrow 0$, and Eq. (13) reduces to $\phi_{\text{eq}} = k\psi_0(\ell)/(1 + k\psi_0(\ell))$, where ϕ_{eq} is the equilibrium fraction of reacted ligands. Using this, one can rewrite Eq. (13) as

$$\hat{\phi}(s) = \frac{\phi_{\text{eq}}}{s} \frac{1}{1 + \phi_{\text{eq}}sh(s)}, \quad (14)$$

where

$$h(s) = \frac{\hat{G}(\ell, \ell, s)}{\psi_0(\ell)} - \frac{1}{s}. \quad (15)$$

Notice that $sh(s)$ vanishes in the limit $s = 0$. The information about the dynamics of the system is contained in the propagator $\hat{G}(\ell, \ell, s)$.

In order to obtain the time variation of the reacted fraction of ligands, $\phi(t)$, one has to perform the Laplace inversion of $\hat{\phi}(s)$. Although the inversion does not always lead to an analytical function, and one might need to resort to numerical Laplace inversion, it is in general straightforward to extract the long time behavior of $\phi(t)$. This follows from the analysis of the poles^{23,29} of Eq. (14), which solve the equation

$$1 + \phi_{\text{eq}}s^*h(s^*) = 0. \quad (16)$$

The longest decay time in $\phi(t)$ is given by the pole that is closest to the origin. Around this pole, the inverse Laplace transform leads to

$$\phi(t) = \phi_{\text{eq}}(1 - \exp[-t/\tau_{\text{re}}]) \quad (17)$$

with characteristic time $\tau_{\text{re}} = 1/|s^*|$.

One can relate τ_{re} to the characteristic time τ_{ir} of a system where the reaction is irreversible ($k \gg 1$). This has the advantage of identifying what are the respective roles of the local bond formation and bond rupture on the final, diffusion

dependent reaction process. In order to obtain τ_{ir} , the time required to irreversibly bind the ligand–receptor pairs, one first solves the following equation:

$$1 + s^{**}h(s^{**}) = 0, \quad (18)$$

which is the analogous of Eq. (16), but with $\phi_{\text{eq}} = 1$, and search once again for the pole s^{**} that is closest to zero. In the limit of large characteristic time scales, when the ligands have to climb a potential barrier larger than $k_B T$ to meet the receptors, s^{**} is almost zero and one can show that, to leading order, $h(0) \approx 1/|s^{**}| = \tau_{\text{ir}}$. From Eq. (16), it follows that $h(0) \approx 1/(\phi_{\text{eq}}|s^*|)$ and consequently

$$\tau_{\text{re}} = \frac{1}{|s^*|} = h(0)\phi_{\text{eq}} = \tau_{\text{ir}}\phi_{\text{eq}}. \quad (19)$$

Notice that the argument above depends on the condition that the reaction times τ_{ir} and τ_{re} are clearly larger than any characteristic microscopic time. For clarity, one finally rewrites Eq. (17) as

$$\phi(t) = \phi_{\text{eq}}(1 - \exp[-t/(\phi_{\text{eq}}\tau_{\text{ir}})]). \quad (20)$$

This shows that the long time behaviors of irreversible and reversible binding are similar, up to a normalization factor of time and ligand fraction. The normalization factor is trivially the equilibrium value of the ligand fraction in the presence of the receptors. Before turning to applications, we connect this equilibrium value ϕ_{eq} to the characteristics of the ligand–receptor bond. As depicted in Fig. 3, $U(\ell)$ is the difference between the minimum of the potential where the ligand is confined and the value of the potential at the receptor site. The ligand has to overcome an energy barrier $U(\ell)$ in order to reach the receptor. The depth of the binding potential at the receptor is given by W (notice that we set $k_B T = 1$). In this simplified model, the larger W is, the stronger is the binding between the ligand and the receptor. Provided that the potential $U(z)$ is convex and that the ligand and the receptor are much smaller than the characteristic length scale of variation of U , one can ignore the details of the confining potential in order to obtain an equilibrium value of bound ligands. Under such conditions, the system behaves approximately like a two state model, where one state has zero potential energy (ligands outside) and the other a potential energy $U(\ell) - W$ (ligands inside). One can easily show that the fraction of bound ligands is related to $U(\ell)$ and W through

$$\phi_{\text{eq}}(\ell) = \frac{e^{W-U(\ell)}}{1 + e^{W-U(\ell)}}. \quad (21)$$

The importance and usefulness of this relation is that it separates the effects of the tether potential, which is solely related to the position of the receptors and the equilibrium binding strength.

A. The cyclization reaction of a single spring

We first study the academic problem of a collection of noninteracting ligands attached to single springs of spring constant κ , in a viscous medium with a friction coefficient ζ and in contact with a thermal bath. The receptor is located at

the origin $z = \ell = 0$ [i.e., $U(\ell) = 0$], and the potential depth is given by W . This is a simplified one-dimensional version of the classical polymer cyclization problem.

By solving the Langevin equation, one can show that for this system the dynamic propagator is given by²²

$$G(z, z', t - t') = \frac{1}{\sqrt{2\pi\lambda^2(1-j^2)}} \exp\left\{-\frac{(z-z'j)^2}{2\lambda^2(1-j^2)}\right\}, \quad (22)$$

where z and z' are the positions of the ligand, respectively, at times t and t' (with $t' < t$), $\lambda = 1/\kappa^{1/2}$ is the characteristic length scale associated with the quadratic potential, in units where $k_B T = 1$, and $j = \exp(-(t-t')/\tau)$. The characteristic microscopic time τ is given by $\tau = \zeta/\kappa$. The dynamic propagator can be equivalently formulated as a conditional probability for the ligand: given its position z' at time t' , it gives the probability of finding the ligand at position z at time t . For completeness, we quickly discuss the two dynamic limits contained in the propagator.

For times much smaller than the characteristic time of relaxation ($t-t' \ll \tau$), $j \approx 1 - (t-t')/\tau$ and the dynamic propagator reduces to

$$G = \exp\{- (z-z')^2/4Dt\} / \sqrt{4\pi Dt}, \quad (23)$$

where $D = 1/\zeta$ is the diffusion constant. As expected at short times, the propagator is that of a free diffusing ligand that does not feel the presence of the confining potential $U(z) = \kappa z^2/2$.

For times much larger than the relaxation time ($t-t' \gg \tau$), where $j \approx 0$ one has

$$G = \exp\{-z^2/2\lambda^2\} / \sqrt{2\pi\lambda^2}. \quad (24)$$

The dynamic propagator has reduced to the Boltzmann distribution: after a long time, the system reaches thermal equilibrium and the probability of finding the ligand at a certain position becomes independent of the initial condition.

In order to obtain $\phi(t)$, the probability of finding the ligand reacted at time t , one needs to determine the function $h(s)$ [cf. Eq. (15)], where G is now given by Eq. (22) and ψ_0 by Eq. (24). One can show that

$$h(s) = \frac{1}{s} \left[\frac{\sqrt{\pi}\Gamma(1+s\tau/2)}{\Gamma(1/2+s\tau/2)} - 1 \right] \quad (25)$$

with $\Gamma(x)$ the usual gamma function.²⁹ This in turn, when plugged into Eq. (14), leads to

$$\hat{\phi}(s) = \frac{\phi_{\text{eq}}}{s} \frac{1}{1 - \phi_{\text{eq}} + \phi_{\text{eq}} \sqrt{\pi}\Gamma(1+s\tau/2)/\Gamma(1/2+s\tau/2)}. \quad (26)$$

In the case of irreversible reactions, the potential well depth W is infinite and $\phi_{\text{eq}} = 1$ [see Eq. (21)], and $\phi(s)$ reduces to

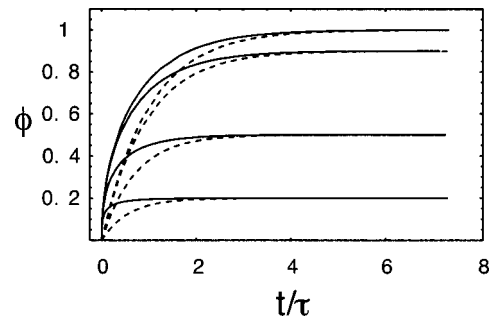


FIG. 1. Time dependence of the fraction of bound ligands ϕ , for $\phi_{\text{eq}} = 1, 0.8, 0.5$, and 0.2 . The full lines correspond to the exact inverse Laplace transform of Eq. (26), obtained analytically for $\phi_{\text{eq}} = 1$ [cf. Eq. (28)], and numerically for the other values of ϕ_{eq} . The dashed lines are the long time behavior from Eq. (17) with the characteristic times following from Eq. (16): $\tau_{\text{re}}/\tau = 1$ for $\phi_{\text{eq}} = 1$, $\tau_{\text{re}}/\tau = 0.94$ for $\phi_{\text{eq}} = 0.9$, $\tau_{\text{re}}/\tau = 0.70$ for $\phi_{\text{eq}} = 0.5$ and $\tau_{\text{re}}/\tau = 0.56$ for $\phi_{\text{eq}} = 0.2$.

$$\hat{\phi}(s) = \frac{1}{s} \frac{\Gamma(1/2+s\tau/2)}{\sqrt{\pi}\Gamma(1+s\tau/2)}. \quad (27)$$

One can show that the latter is the Laplace transform of the function

$$\phi(t) = 1 - \frac{2}{\pi} \arcsin(\exp(-t/\tau)). \quad (28)$$

This provides an interesting case where an exact Laplace inversion can be performed. Figure 1 shows $\phi(t)$ as in Eq. (28) and the corresponding long time behavior as given by Eq. (17). Notice that in this particular case, the characteristic reaction time τ_{ir} is the same as the microscopic time τ . Figure 1 also shows $\phi(t)$ obtained through numerical Laplace inversion³⁰ of Eq. (26) for different values of $\phi_{\text{eq}} \neq 1$, as well as the corresponding long time behavior given by Eq. (17). As expected, the long time behavior agrees with the exact results at $t/\tau \gg 1$.

Another informative quantity to compute, is the single ligand spacial distribution $\psi(z, t)$. In order to obtain it, one can use the fact that Eq. (12) is the Laplace transform of

$$\frac{d\phi(t)}{dt} = q\psi(\ell, t) - p\phi(t) \quad (29)$$

[with $\phi(0) = 0$]. One can then rewrite the reaction-diffusion Eq. (8) as

$$\psi(z, t) = \psi_0(z) - \int_0^t dt' G(z, \ell; t-t') \frac{d\phi(t')}{dt'}. \quad (30)$$

For the irreversible case, one has the analytical form of $\phi(t)$, and naturally its derivative. After some algebra one can show that

$$\psi(z, t) = \frac{1}{\sqrt{2\pi\lambda^2}} \left\{ \exp(-z^2/2\lambda^2) - \frac{2}{\pi} \int_j^1 dj' \frac{\exp(-z^2/2(1-(j/j')^2))}{\sqrt{(1-j'^2)(1-(j/j')^2)}} \right\}, \quad (31)$$

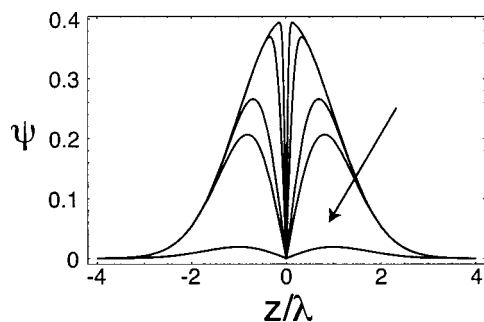


FIG. 2. The time variation of the probability distribution of a ligand diffusing in quadratic potential. At $t=0$ the ligand is in thermal equilibrium [with $\psi(z/\lambda) \sim \exp[-z^2/(2\lambda^2)]$], and an infinite well is put at the origin. As time goes on, the probability of finding the ligand outside the well (i.e., the integral of ψ) decreases. The snapshots of ψ are taken at $t=0.999\tau$ (probability almost 1 of finding the ligand outside the well), 0.9τ , 0.9τ , 0.8τ , and 0.1τ (probability almost 0 of finding the ligand outside the well). The arrow indicates the time evolution of the successive curves.

where $j = \exp(-t/\tau)$. The time evolution of $\psi(z, t)$ is shown in Fig. 2. As expected, the reaction first concerns those ligands which were close to the receptors. As some of the ligands are removed from the distribution, others diffuse into the reaction zone and are consumed as well. As time goes to infinity, no ligands are left outside the well, and the distribution function vanishes.

B. Receptor away from the origin: The Kramers problem

We now consider the model usually employed to model tethered ligand–receptor interactions, with the ligand attached to a single spring of constant κ and the receptor on the opposing surface at $z = \ell \neq 0$. In this case, the function $h(s)$ for the quadratic potential is given by

$$h(s) = \int_0^\infty dt \exp(-st) \left[\frac{\exp((\ell/\lambda)^2 j / (1+j))}{\sqrt{1-j^2}} - 1 \right], \quad (32)$$

where again $j = \exp(-t/\tau)$. The solution of Eq. (18) using the $h(s)$ above leads to the relevant τ_{ir} . If the receptor is in a position such that $U(\ell)$ (cf. Fig. 3) is larger than $k_B T$, one

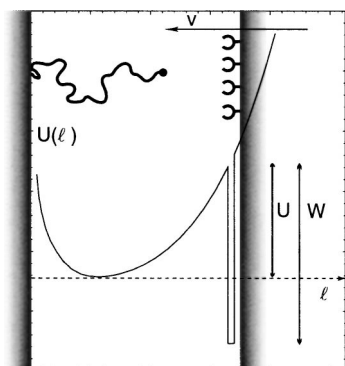


FIG. 3. Idealization of the SFA experiments. A functionalized polymer (containing a ligand in one of its ends) attached to a surface creates the potential felt by the ligand. A second surface is homogeneously covered by receptors. The two surfaces approach each other at speed v .

can show that

$$\frac{\tau_{ir}}{\tau} = \frac{1}{|s^{***}|} \approx \frac{\sqrt{2\pi}\lambda}{\ell} \exp((\ell/\lambda)^2/2). \quad (33)$$

The reaction time is here an exponential function of the position of the receptor, the classical Kramers result for the first passage problem,³¹ of a ligand escaping over the barrier of a quadratic potential into an infinitely deep and steep adhesion well.

III. SPECIFIC ADHESION PROMOTED BY LIGAND–RECEPTOR PAIRS

A. Specific binding of approaching surfaces

There has been recently an increasing interest in the adhesion between surfaces through interacting ligand–pair receptors.^{16–18} Although a large amount of theoretical work has been devoted to the problem of rupture between such surfaces, surprisingly not much has been done on the problem of spacer-mediated specific adhesion between two approaching surfaces. The tools presented in the preceding section are ideal to describe theoretically such systems. Recent experiments^{16,17} on such systems yielded some intriguing results. Figure 3 sketches an idealized surface force apparatus (SFA) experiment: functionalized polymers, which contain at one end a chemically bound ligand molecule (e.g., biotin), are attached to a plane; the surface coverage by polymers is low, i.e., the polymers hardly interact with each other. In an opposing plane, the receptors (e.g., streptavidin) are homogeneously distributed. The number of available receptors is much larger than the number of ligands. In the language of the preceding section, the ligand moves in a potential, which is created by the polymer and, when in contact with a receptor, reacts reversibly to form a complex. The depth of the ligand–receptor potential W can be taken from experimental data (cf. Table I). In the SFA experiments, the two surfaces approach each other roughly at a constant speed v , of the order of 1 Å/s, and the force exerted by one surface on the other is measured. When the slope of the force, i.e., when the derivative of the force with respect to distance between surfaces, becomes larger than the spring constant of the SFA apparatus, the system becomes unstable and the two surfaces jump into contact.

The knowledge of the fraction of bound ligands, or equivalently bridging chains, at a certain time allows the calculation of the force between the surfaces. Since the polymers are assumed to not interact with each other, simply summing the forces exerted by each of the bound polymer leads to a force law that can be directly compared to experiments. For this reason, the reaction–diffusion formalism is useful in this context, but one still needs to have a reasonable description for the dynamic propagator of the polymer attached to a wall. This is an unresolved question in polymer science:³² for describing the experimental system some approximation to τ_{ir} needs to be done. If for instance the polymer could be described by a single harmonic spring, the ligand would then diffuse in a simple harmonic potential, leading in the limit of large ℓ , the distance between the surfaces, to the irreversible reaction time given in Eq. (33). This

is however a poor approximation. A more realistic description can be obtained through the Rouse model, which accounts for all the internal modes of the end-attached chain but not for the presence of the neighboring impenetrable wall. In this case, the propagator still has the Gaussian form, Eq. (22), but the relaxation function $j(t)$ is now a sum of many modes.²³ One can show in this case that¹⁷

$$\tau_{\text{ir}}(\ell) = \frac{\tau_R \pi^{7/2}}{8U(\ell)^{3/2}} \exp\{U(\ell)\}, \quad (34)$$

while the Zimm model, which includes hydrodynamic interactions,²² gives

$$\tau_{\text{ir}}(\ell) = \frac{\tau_Z 1.43}{U(\ell)} \exp\{U(\ell)\}, \quad (35)$$

within the preaveraging approximation.²² τ_R and τ_Z are, respectively, the Rouse and the Zimm times. In this work we will use τ_{ir} from the Zimm model, which is more appropriate for dilute polymer solutions. Note also that the reaction time obtained from the Rouse model is a factor U faster than the time obtained from a single spring. This reflects the compact space exploration²⁷ of the movement of the chain end. The Zimm result is still faster by a factor $U^{1/2}$ than the spring result, but slower by a factor $U^{1/2}$ than the Rouse result.

Using the Rouse or the Zimm model allows for a proper treatment of the multimode nature of the chain motion, to within the limits of the assumed model. However, any of these models refer intrinsically to Gaussian chain models, which do not lead to the proper landscape of the extension energy $U(\ell)$. In order to improve our predictions, we had recourse of Monte Carlo simulations to produce a more realistic stretching potential $U(\ell)$. Simulations for a pearl-bead model of a chain between two walls were performed and the resulting force-distance and energy-distance profiles obtained. These results, published elsewhere,¹⁷ will be used here. Notice that these simulations reveal that the large extension limit ($\ell/aN > 0.7$) for the stretching energy follows a law similar to that of the freely jointed chain (FJC) model, albeit with a different prefactor:

$$U(\ell) \approx -N \log \left[2.15 \left(1 - \frac{\ell}{aN} \right) \right], \quad (36)$$

where N is the number of Kuhn units and a the Kuhn length.

Finally, we still have to modify the results obtained in Sec. II in order to accommodate for the fact that the surfaces actually move with respect to one another. With Eq. (17) one is able to calculate the variation of the fraction of chains that bridge between two such immobile surfaces as a function of time. Naturally, it is more useful to calculate the fraction of bridging chains as a function of the distance ℓ between two moving surfaces. From this one can easily calculate the force as a function of the distance, and one can also easily extract the range of interaction ℓ_r .

One can easily go from one description to the other in the case where the surfaces move in respect to each other with a velocity v much smaller than $v^* = R_F/\tau_Z$, where $R_F = N^{3/5}a$ is the Flory radius of the polymer and $\tau_Z = \eta R_F^3/k_B T$ is the Zimm time (which is the characteristic microscopic time in this problem, where η is the solvent viscosity). For relatively short chains (with the number of Kuhn units of the order 100) this velocity corresponds to $\sim 10^9$ Å/s, which is much larger than the usual experimental values for v . In this limit, one can apply the chain rule to $d\phi(t)/dt$ and obtain

$$\frac{d\phi(t)}{dt} = -v(\ell) \frac{d\phi(\ell)}{d\ell}, \quad (37)$$

where $v(\ell) = d\ell(t)/dt$, which assumes a unique and invertible relation between the distance between the surfaces and time, viz. $\ell(t)$. The left-hand side (lhs) of Eq. (37) is given by the time derivative of Eq. (20), which can be rewritten as

$$\frac{d\phi(t)}{dt} = \frac{\phi_{\text{eq}}(\ell(t)) - \phi(\ell(t))}{\phi_{\text{eq}}(\ell(t)) \tau_{\text{ir}}}. \quad (38)$$

Note that ϕ_{eq} depends on the distance ℓ between the surfaces through its dependence on $U(\ell)$, as in Eq. (21). One can now eliminate the time variable from the problem, and obtain the differential equation

$$\frac{d\bar{\phi}(\ell)}{d\ell} - \frac{\bar{\phi}(\ell)}{v(\ell) \phi_{\text{eq}}(\ell) \tau_{\text{ir}}} = \frac{d\phi_{\text{eq}}(\ell)}{d\ell}, \quad (39)$$

where $\bar{\phi}$ is, as wished, the free parameter and $\bar{\phi} \equiv \phi_{\text{eq}}(\ell) - \phi(\ell)$ is the function we would like to know. The boundary condition for Eq. (39) is that at $\ell \rightarrow \infty$, $\bar{\phi}(\ell \rightarrow \infty)$ vanishes, since both the fraction of bound chains ϕ and the equilibrium value ϕ_{eq} vanish in this limit. Solving the differential equation finally leads to

$$\phi(\ell) = \int_{\ell}^{\infty} d\ell'' \left(-\frac{d\phi_{\text{eq}}(\ell'')}{d\ell''} \right) \left(1 - \exp \left\{ -\int_{\ell}^{\ell''} \frac{d\ell'}{v(\ell') \phi_{\text{eq}}(\ell') \tau_{\text{ir}}(\ell')} \right\} \right) \quad (40)$$

which gives the fraction of bound chains as a function of the distance ℓ between them as the two surfaces approach at a speed $v(\ell)$ assumed much smaller than the microscopic speed v^* . When the latter assumption is not true, for high speeds of approach, the problem has to be reformulated at the level of the reaction-diffusion Eq. (8) to take into account the relative movement of the surfaces.

With Eq. (40) one is finally in a position where a system as the one depicted in Fig. 3 can be theoretically analyzed. Figure 4 shows the fraction of bound chains for a chain of 100 monomers, $N = 100$ (with monomer size $a = 3.5$ Å, and $R_F = 66$ Å), both for a given adhesion strength W at various speeds of approach and at constant speed for various values of the adhesion strength W . As previously mentioned, the

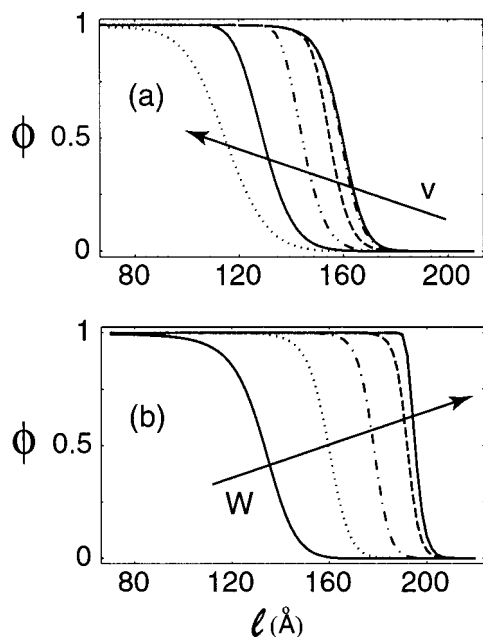


FIG. 4. Fraction of bound chains ϕ as a function of the distance between surfaces ℓ (for $N=100$ and equilibrium size $R_F=66$ Å). Plot (a), fixed adhesion strength $W=10 k_B T$ for speeds (from right to left) $v=1, 10^4, 10^5, 10^6, 10^7$, and 5×10^7 Å s $^{-1}$. The two lower speeds are coincident, indicating that for this chain and affinity, equilibrium conditions are reached for $v < 10^4$ Å s $^{-1}$. Plot (b), fixed speed $v=1$ Å s $^{-1}$ and affinity (from left to right) $W=5, 10, 15, 20, 25$, and $30 k_B T$. For $W > 20$ the curves coincide, indicating that irreversible conditions are at work.

potential $U(\ell)$ created by the polymer, present both in the expression for ϕ_{eq} and τ_{ir} , was obtained elsewhere through MC simulations.¹⁷ As it can be seen from Fig. 4(a), an experiment performed at a small enough speed v allows the system to reach the equilibrium value of ϕ , while increasing speeds reduce the interaction range by a substantial amount. In this latter situation the chains do not have the time to reach across the gap into their equilibrium range position before the surfaces move into a smaller distance. For the case shown in the figure, with $N=100$ and $W=10 k_B T$, speeds superior to 5×10^3 Å s $^{-1}$ result in a significant reduction of the adhesion range from its equilibrium value at $\ell_{eq} = 160$ Å. Given a typical experimental speed of 1 Å s $^{-1}$, Fig. 4(b) shows when the adhesion strength value W is high enough for the adhesion range to be independent of the actual W value, a situation we refer to as irreversible adhesion.

The importance of the speed of approach v and of the adhesive strength W is summarized in Fig. 5. For simplicity, we define the range of adhesion the distance ℓ_r between the surfaces at which half of the chain bridge, i.e., $\phi(\ell_r) = 1/2$. There is nothing fundamental about this definition, and depending on the particular experimental setup, this definition has to be modified. The adhesion range ℓ_r of a polymeric tether with $N=100$ is shown in Fig. 5(a) as a function of the speed of approach v , for fixed values of adhesive strength W , while in Fig. 5(b) ℓ_r is shown as a function of the binding strength W (for fixed values of v). At large enough values of v or W , the range becomes independent of the binding strength but becomes (weakly) dependent on the speed of approach, a fact that is reflected in the crossover line which

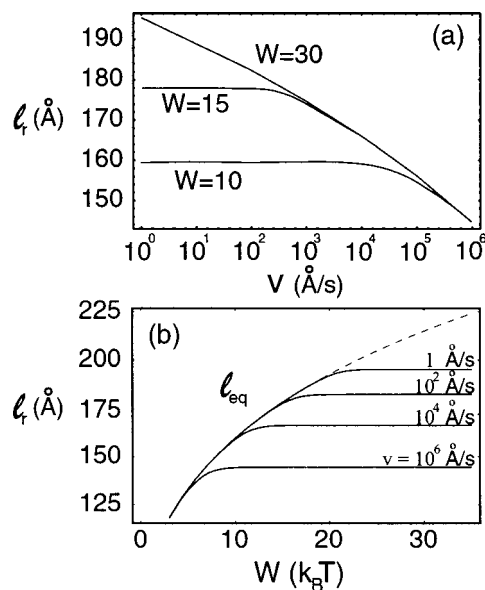


FIG. 5. The behavior of the adhesion range as a function of the speed of approach v (top) and binding strength W (bottom). Plot (a), ℓ_r as a function of the speed of approach v for fixed values of the strength W . At low enough speed of approach v the range is determined by the equilibrium condition $U(\ell_{eq})=W$. Plot (b), ℓ_r as a function of the adhesive strength W (for $N=100$). At small enough binding strength, the equilibrium range of interaction ℓ_{eq} is again recovered (dashed curve). Notice that in both graphs the nonequilibrium behavior sets in at high speed v and at high binding strength W .

divides the limits of equilibrium from irreversible adhesion, as depicted in Fig. 6.

Finally, the index of polymerization of the polymer tethers and the strength of the ligand–receptor couples can be experimentally varied in an independent way, thus tuning the range of adhesion. We plot in Fig. 7 the interaction range for a variety of chain lengths and fixed adhesion strength $W = 25 k_B T$, at various approaching speeds. As expected, lower speeds and longer chains have larger adhesion range. Note also the concavity of the curves showing that longer chains bridge at smaller relative extensions than the shorter ones.

B. Rupture of specifically bounded surfaces

The formalism shown above can be equally applied to the case where two bound surfaces are moved away from each other (i.e., rupture). The chain rule in Eq. (37) now reads

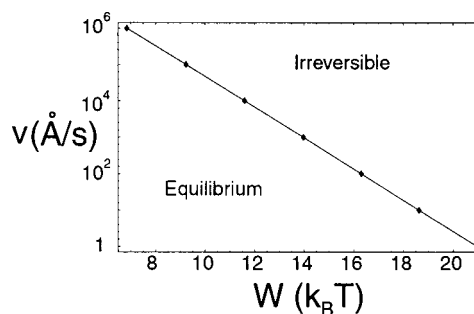


FIG. 6. The crossover line from reversible to irreversible adhesion (given by the point where ℓ_{eq} equals the plateau value of ℓ_r at a given v).

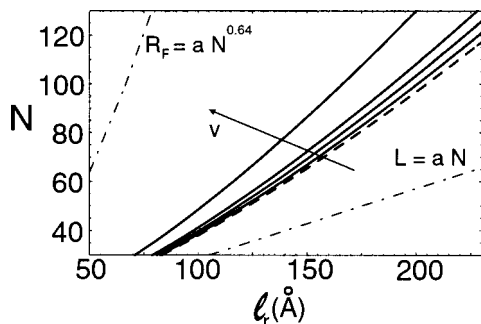


FIG. 7. Range of adhesion ℓ_r for polymers with different indices of polymerization N ($a=3.5$ Å and $W=25 k_B T$). The dashed curve is the equilibrium solution (equivalent to $v=0$), and the full curves correspond, from right to left, to $v=0.1, 1, 10$, and 10^4 Å/s. The dotted-dashed curves correspond to the total extension of the polymer and the equilibrium end positions.

$$\frac{d\phi(t)}{dt} = v(\ell) \frac{d\phi(\ell)}{d\ell}. \quad (41)$$

Using the latter and similar manipulations that followed Eq. (37), one arrives at (now with boundary condition $\phi=1$ as $\ell \rightarrow 0$)

$$\phi(\ell) = 1 + \int_0^\ell d\ell'' \left(\frac{d\phi_{\text{eq}}(\ell'')}{d\ell''} \right) \times \left(1 - \exp \left\{ - \int_{\ell''}^\ell \frac{d\ell'}{\ell'' v(\ell') \phi_{\text{eq}}(\ell') \tau_{\text{ir}}(\ell')} \right\} \right). \quad (42)$$

Away from equilibrium, i.e., at high enough speed v , the behavior of $\phi(\ell)$ strongly depends on whether the two surfaces approach or move away from each other. As depicted in Fig. 8, when the two surfaces move apart from each other at high enough speeds, the bounded ligand-receptor pairs do not have the time to unbind at the equilibrium range, leading to an effective increase of the range of adhesion in comparison to the equilibrium value. This is exactly the opposite effect as in the case where the surfaces approach each other: at high enough v , $\phi(\ell)$ exhibits a hysteresis (cf. inset to Fig. 9), leading to different values of ℓ_r if the surfaces are approaching or moving away from each other (at the same speed v). This is explicitly shown in Fig. 9, where the range

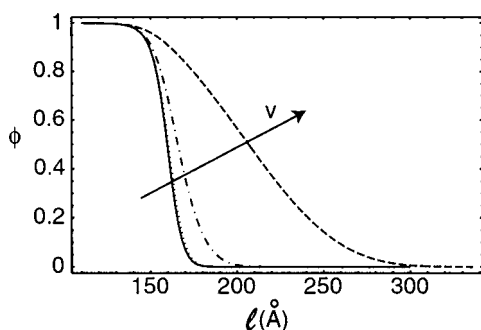


FIG. 8. Fraction of bound chains ϕ as a function of the distance between surfaces ℓ (for $N=100$ and equilibrium size $R_F=66$ Å) and fixed adhesion strength $W=10 k_B T$ for speeds (from right to left) $v=1, 10^4$ (indistinguishable from the former), 10^5 and 10^6 Å/s. Notice that the evolution of the curves occurs in the opposite order as in the case of approaching surfaces.

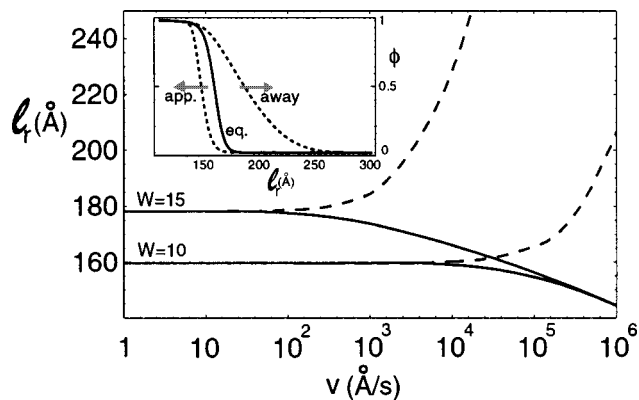


FIG. 9. Range of adhesion as a function of the speed v for two surfaces approaching (full lines) and moving away (dashed lines) from each other (for $W=10$ and $W=15 k_B T$). In equilibrium, ℓ_r does not distinguish the direction of v . Away from equilibrium, the range of adhesion for surfaces approaching each other is always smaller than for surfaces moving away from each other due to the hysteresis exhibited by $\phi(\ell)$ (shown as the inset for $v=5 \times 10^5$ and $W=10$).

of adhesion is plotted as a function of v (for $W=10$ and $W=15$) for both approaching and receding surfaces.

Finally, we calculate the dynamic strength between the two surfaces during the rupture process. Although these results are already known in the literature (see, for instance, Refs. 12 and 15), it is of interest to check the results that the reaction-diffusion formalism yield. At a certain distance ℓ , the force exerted by each chain is given by $f(\ell) = -dU(\ell)/d\ell$. For the planar geometry considered in Fig. 3, it follows that the total statistical (average) force exerted by one surface on the other is given by $F(\ell) = f(\ell)\phi(\ell)$. As it is shown in Fig. 10, this force increases in range, as previously discussed, but also in magnitude. The force shows a nonmonotonic behavior, and its maximum value is usually associated to the critical force necessary to pull apart the two surfaces. At low speeds the critical force has been shown¹⁵ to scale linearly with v , a behavior that we also obtain, as Fig. 11 shows. The formalism used here is thus consistent with previous results, but we argue that it has a wider range of application and it is liable to several developments accounting for instance for heterogeneous distributions of receptors or solvent flow.

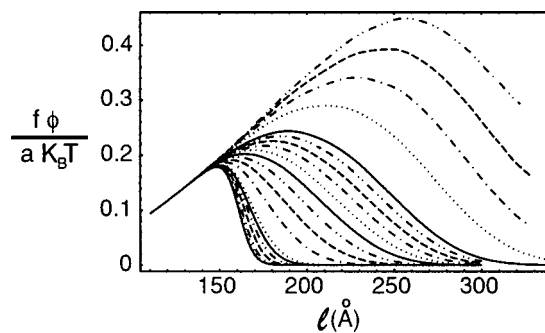


FIG. 10. Force (dynamic strength) between two surfaces during rupture. The various curves represent velocities v between the surfaces varying, from bottom to top, between 1 Å/s and 10^7 Å/s. The tethers have $N=100$ units ($R_F=66$ Å) and the binding strength is $W=10 k_B T$. Away from the equilibrium values, the force increases in magnitude and in range with the velocity. The monomer size is given by $a=3.5$ Å.

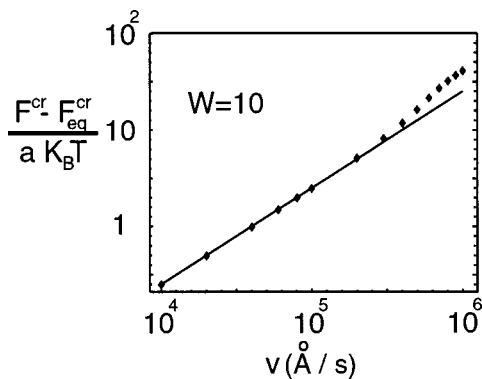


FIG. 11. Critical force (obtained from the maxima in Fig. 10) between two surfaces moving away from each other at velocity v . At low v , the critical force increases linearly with the velocity. The tethers have $N=100$ units ($R_F=66$ Å) and the binding strength is $W=10 k_B T$. The monomer size is given by $a=3.5$ Å.

IV. CONCLUSIONS

In summary, we presented the reaction–diffusion (RD) formalism and applied it to systems where ligands diffusing through a medium can react both reversibly and irreversibly to a receptor. We analyzed in detail the case where the system consists of a ligand in a quadratic potential with a receptor at the origin, both for irreversible as well as for reversible reactions. For the former case, we obtained analytical results for the probability of finding the ligand unreacted, and numerically the time evolution of its spatial probability distribution. We also obtained analytically the long time behavior of the probability of finding the ligand unreacted, and found perfect agreement with numerical results for both irreversible and reversible reactions. We also applied the RD formalism to the case where the ligand moves in a quadratic potential but the receptor is away from the origin, and recovered the classical result first obtained by Kramers. Finally, we used the long time behavior obtained with the RD formalism to determine the properties of specific adhesion between two planar surfaces, both in the cases where these move towards each other (binding) and when these move away from each other (rupture).

The results obtained here for two approaching surfaces are in agreement with experimental results,¹⁷ while the results obtained for the rupture are consistent with previously obtained theoretical results. This formalism is the natural candidate to treat this class of problems, where diffusion and reaction between particles occur. It is also possible to include hydrodynamic flow in the formalism,³³ which can be used, for instance, in the theoretical study of specific adhesion between leukocytes and the endothelial lining in blood vessels. Although the formalism was proposed within the context of tethered ligands–receptor adhesion, one can apply it to study

the problem of friction between surfaces to which polymers are attached³⁴ as well as to transient polymer networks and polymer surfactant mixtures.

ACKNOWLEDGMENTS

The authors thank A. Likhtman, T. Kuhl, and J. Wong for helpful discussions. This work was supported by the Chemistry Department of the CNRS, under AIP “Soutien aux Jeunes Equipes” and by a grant from the France Berkeley Fund. It was also supported in part by the NSF under the MRSEC program award No. DMR00-80034.

- ¹P. Bongrand, *Rep. Prog. Phys.* **62**, 921 (1999).
- ²G. Weber, *Adv. Protein Chem.* **29**, 1 (1975).
- ³P. S. Stayton *et al.*, *Biomol. Eng.* **16**, 39 (1999).
- ⁴C. Yuan, A. Chen, P. Kolb, and V. T. Moy, *Biochemistry* **39**, 10219 (2000).
- ⁵E. Florin, V. T. Moy, and H. E. Gaub, *Science* **264**, 415 (1994).
- ⁶R. Merkel *et al.*, *Nature (London)* **397**, 50 (1999).
- ⁷B. Alberts *et al.*, *Molecular Biology of the Cell*, 3rd ed. (Garland, New York, 1994).
- ⁸G. I. Bell, *Science* **200**, 618 (1978).
- ⁹D. A. Hammer and M. Tirrell, *Annu. Rev. Mater. Sci.* **26**, 651 (1996).
- ¹⁰E. Raphaël and P. G. de Gennes, *J. Phys. Chem.* **96**, 4002 (1992).
- ¹¹A. Kloboucek, A. Behrisch, J. Faix, and E. Sackmann, *Biophys. J.* **77**, 2311 (1999).
- ¹²E. Evans and K. Ritchie, *Biophys. J.* **72**, 1541 (1997).
- ¹³E. Evans and K. Ritchie, *Biophys. J.* **76**, 2439 (1999).
- ¹⁴T. R. Weikl, D. Andelman, S. Komura, and R. Lipowsky, *Eur. Phys. J. E* **8**, 59 (2002).
- ¹⁵U. Seifert, *Europhys. Lett.* **58**, 792 (2002).
- ¹⁶J. Y. Wong *et al.*, *Science* **275**, 820 (1997).
- ¹⁷C. Jappesen *et al.*, *Science* **293**, 465 (2001).
- ¹⁸J. Wong, A. Chilkoti, and V. Moy, *Biomol. Eng.* **16**, 45 (1999).
- ¹⁹G. I. Bell, M. Dembo, and P. Bongrand, *Biophys. J.* **45**, 1051 (1984).
- ²⁰M. Dembo, D. C. Torney, K. Saxman, and D. A. Hammer, *Proc. R. Soc. London N* **45**, 58 (1988).
- ²¹C. Zhu, *J. Biomech.* **33**, 23 (2000).
- ²²M. Doi and S. F. Edwards, *The Theory of Polymer Dynamics* (Clarendon, Oxford, 1986).
- ²³M. Doi, *Chem. Phys.* **11**, 107 (1975).
- ²⁴A. G. Moreira, C. Jeppesen, F. Tanaka, and C. M. Marques, *Europhys. Lett.* **62**, 876 (2003).
- ²⁵H. Risken, *The Fokker-Planck Equation: Methods of Solution and Applications*, 2nd ed. (Springer, Berlin, 1996).
- ²⁶G. Arfken, *Mathematical Methods for Physicists*, 3rd ed. (Academic, San Diego, 1985).
- ²⁷P. G. de Gennes, *J. Chem. Phys.* **76**, 3316 (1982).
- ²⁸It was first brought to our attention by A. Likhtman that the reaction–diffusion solution presented here, first introduced by Doi and de Gennes, is not a general solution of the reaction–diffusion problem for polymers. It does provide the right values for the cases discussed in this paper, but it fails for instance for the case of polymer cyclization, where it leads to the right scaling form of the cyclization time but not to the exact prefactor. This will be discussed in a forthcoming paper by A. Likhtman.
- ²⁹M. Abramowitz and I. A. Stegun, *Handbook of Mathematical Functions* (Dover, New York, 1974).
- ³⁰For the numerical Laplace inversion we used Arnaud Mallet’s package for Mathematica available at www.wolfram.com
- ³¹H. A. Kramers, *Physica (Utrecht)* **7**, 284 (1940).
- ³²M. Koch, J. Sommer, and A. Blumen, *J. Chem. Phys.* **106**, 1248 (1997).
- ³³A. Kolb, C. M. Marques, and G. H. Fredrickson, *Macromol. Theory Simul.* **6**, 169 (1997).
- ³⁴T. Charitat and J. Joanny, *Eur. Phys. J. E* **3**, 369 (2000).